Biotinylated surfome profiling identifies potential biomarkers for diagnosis and therapy of *Aspergillus fumigatus* infection

Lei-Jie Jia[1], *Thomas Krüger*[1], *Matthew G. Blango*[1], *Olaf Kniemeyer*[1,2]*, *Axel A. Brakhage*[1,2]*

[1] Department of Molecular and Applied Microbiology, Leibniz Institute for Natural Product Research and Infection Biology—Hans Knöll Institute, Jena, Germany.

[2] Department of Microbiology and Molecular Biology, Institute of Microbiology, Friedrich Schiller University, Jena, Germany.

*Correspondence:

E-mail: olaf.kniemeyer@leibniz-hki.de (OK); axel.brakhage@leibniz-hki.de (AAB)

Tel: +49 (0)3641-532 1071 (OK); +49 (0)3641-532 1001 (AAB)

ABSTRACT

Aspergillus fumigatus is one of the most common airborne fungi capable of causing invasive mycoses in immunocompromised patients and allergic diseases in susceptible individuals. In both cases, fungal surface proteins mediate the first contact with the human immune system to evade immune responses or to induce hypersensitivity. Several methods have been established to study the surface proteome (surfome) of *A. fumigatus*, like trypsin shaving, glucanase treatment,

or formic acid extraction. Biotinylation coupled with LC-MS/MS identification of peptides is a particularly efficient method to identify the surface exposed regions of proteins that potentially mediate interaction with the host. After biotinylation of surface proteins during spore germination, we detected 314 different surface proteins, including several well-known proteins like RodA, CcpA, and DppV, as well as several allergens, heat shock proteins (HSPs), and previously undescribed surface proteins. Using immunofluorescence microscopy, we confirmed the surface localization of three HSPs, which may have moonlighting functions. Collectively, our study generated a comprehensive data set of the *A. fumigatus* surfome, which complements already existing *A. fumigatus* surface proteome data and allows us to propose a common core set of *A. fumigatus* surface proteins. In addition, our study uncovers the surface-exposed regions of many proteins on the surface of spores or hyphae. These surface exposed regions are candidates for direct interaction with host cells and may represent antigenic epitopes that either induce protective immune responses or mediate immune evasion. Thus, the comprehensive datasets provided and compiled here represent reasonable immunotherapy and diagnostic targets for future investigations.

HIGHLIGHTS

- Surface protein biotinylation coupled with LC-MS/MS analysis provides a comprehensive dataset of the *A. fumigatus* surface proteome.
- 314 different *A. fumigatus* proteins (including immunoreactive proteins, and virulence factors) with surface exposed regions were detected.
- Surface localization of three Hsp70 chaperones was confirmed by protein tagging coupled with immunofluorescence.

• By comparison with other surfome datasets, a core surfome of *A. fumigatus* was defined, which provides possible biomarkers for diagnosis or therapy.

SIGNIFICANCE

Aspergillus fumigatus is the most important airborne human pathogenic mold, capable of causing both life-threatening invasive pulmonary aspergillosis in immunocompromised patients and allergic infections in atopic individuals. Despite its obvious medical relevance, timely diagnosis and efficient antifungal treatment of *A. fumigatus* infection remains a major challenge. Proteins on the surface of conidia (asexually produced spores) and mycelium directly mediate host-pathogen interaction and also may serve as targets for diagnosis and immunotherapy. However, the similarity of protein sequences between *A. fumigatus* and other organisms, and sometimes even the human host, makes selection of targets for immunological-based studies difficult. Here, using surface protein biotinylation coupled with LC-MS/MS analysis, we identified hundreds of *A. fumigatus* surface proteins with exposed regions, further defining putative targets for possible diagnostic and immunotherapeutic design.

KEYWORDS

Aspergillus fumigatus, surface biotinylation, surfome, LC-MS/MS, allergens, heat shock protein.

1. INTRODUCTION

The saprotrophic fungus *Aspergillus fumigatus*, which occurs on decaying organic material, is associated with a wide spectrum of diseases in humans [1, 2]. The inhalation of *A. fumigatus* airborne conidia may cause life-threatening invasive pulmonary aspergillosis in

immunocompromised patients, chronic pulmonary aspergillosis in immunocompetent patients with underlying lung diseases, or allergic infections such as allergic bronchopulmonary aspergillosis (ABPA) in atopic individuals [3, 4]. Despite continuous research and improvements of diagnostic tools, timely diagnosis of *A. fumigatus* remains a challenge [2]. Detection kits for a few different recombinant allergens of *A. fumigatus* are now commercially available for the diagnosis of ABPA, but cross-reactivity with antigens from other microorganisms still makes diagnosis difficult [5]. In addition to DNA and cell wall polysaccharides, fungal proteins exposed to the surface may serve as candidate diagnostic markers and valuable targets for new therapeutics [6, 7].

The *A. fumigatus* cell wall not only maintains cellular integrity and protects from external aggression, but it also serves as a harbor for virulence factors that contribute to immune evasion, adherence, and virulence [8]. Although the cell wall is composed of <10% proteins [2] and hundreds of surface proteins have been detected across various proteome studies [9-11], only a few of these proteins are well characterized, including their roles in *A. fumigatus* virulence. RodA, which forms the hydrophobic rodlet layer on dormant conidia, is the best-studied conidial surface protein. RodA is immunologically inert and can mask dectin-1- and dectin-2-dependent host responses [12, 13]. Despite this important role, a rodletless mutant showed no attenuation in virulence in a mouse infection model of invasive aspergillosis [14]. Another abundant conidial surface protein, CcpA, presumably plays a role in maintaining the spore surface structure and preventing immune recognition. Consequently, it was shown to be essential for virulence in a corticosteroid immunosuppressed mouse infection model [10]. The *A. fumigatus* protein CalA, which is present on swollen conidia and germlings, acts as an invasin through interaction with integrin $\alpha_5\beta_1$ on host cells and is required for full virulence and lung invasion in corticosteroid-

treated mice [15]. Beside these virulence determinants on the conidial surface, many allergens are also surface exposed. Asp f 2 has been described as a zinc acquiring protein and is one of the major allergens of *A. fumigatus* [16]. It was found to bind laminin and IgE antibodies from patients with ABPA [17]. Asp f 2 acts as an immune evasion protein by binding human plasma regulators, which leads to inhibition of opsonization and damage of human lung epithelial cells [18]. However, most of the surface exposed proteins are still uncharacterized, and a comprehensive picture of the *A. fumigatus* surface proteome is lacking, but necessary for a better understanding of the interaction of *A. fumigatus* conidia with the host.

Several proteomic studies have already been performed to define the proteins associated with the cell surface of *A. fumigatus*. These studies relied on either strong acids like formic or hydrofluoric acid (HF) or enzymatic treatments with 1,3-β-glucanase or trypsin to release surface proteins for detection [9, 10, 19]. Around 300 common proteins were detected in formic acid extracts of dormant *A. fumigatus* conidia, while the number significantly increased in *A. fumigatus* mutants lacking either the conidial rodlet-layer or the cell wall polymer, α-1,3-glucan [9]. The combined approach of HF-pyridine extraction and trypsin shaving revealed 477 different proteins on dormant or swollen conidia [10], while 178 different proteins were detected on the surface of *A. fumigatus* conidia during germination using the trypsin shaving approach [11]. In addition, the trypsin shaving approach also showed that the composition of the conidial surface proteome is shaped by the sporulation conditions, such as time and temperature [11].

All the aforementioned methods efficiently extract surface proteins and/or peptides, but they also come with drawbacks: they partially disrupt the surface layer and potentially release cell wall-embedded and cytosolic proteins and peptides in addition to their target cell surface proteins. Cell surface biotinylation has been shown to yield the lowest rate of contamination by

cytoplasmic proteins [20] and provides useful information about the surface-exposed protein regions.

Here, we used a widely applied amine-reactive biotinylation method for surface proteomics [15, 21, 22], to label the exposed lysine or N-terminal amino acid residues of *A. fumigatus* cell surface proteins. Subsequently, LC-MS/MS analysis was applied to detect streptavidin-enriched proteins and to define surface-exposed regions based on lysine modifications. The surface localization of several detected proteins was verified through immunofluorescence of Myc-tagged transformants of *A. fumigatus.* Our study complements the picture of the *A. fumigatus* surface proteome and reveals surface proteins that may serve as detection markers or targets for immunotherapy in the future. Perhaps most importantly, we identify a number of proteins that are likely directly involved in the interaction of *A. fumigatus* and the human host.

2. MATERIALS AND METHODS

2.1 Fungal strains and cultivation.

All strains used in this study are listed in Table S1. *A. fumigatus* CEA10 was cultivated as described previously [11]. Briefly, the CEA10 strain was inoculated on *Aspergillus* minimal medium agar plates with 1% (w/v) glucose for 7 days at 37°C. Conidia were harvested in sterile H_2O and separated from hyphae and conidiophores by filtering (30 µm, MACS®). For germination of swollen conidia, 1×10^{10} freshly collected conidia were incubated shaking in 50 mL RPMI 1640 (Lonza) for 5 hours (h) at 37°C. 1×10^{9} conidia were germinated at the same condition for 8 h to enrich for germlings, and 1×10^{9} conidia in 100 mL RPMI 1640 for 14 h to enrich for hyphae.

2.2 Biotinylation of surface proteins.

Experiments were performed as described previously with minor modification [22]. Conidia, germlings, and hyphae were washed three times with PBS (pH 7.4) and then incubated in 5 mL of PBS containing 5 mg EZ-Link Sulfo-NHS-LC-Biotin (Thermo Fisher Scientific, 21335) for 1 h at 4°C. The reaction was terminated by adding two volumes of 100 mM Tris-HCl, pH 7.4 and incubated further for 30 min. The samples were then washed another three times with PBS (pH 7.4).

2.3 Protein extraction and purification.

After adding 1 mL of PBS (pH 7.4) containing protease inhibitor (1 tablet per 10 mL, Roche cOmplete™, #04693159001) and 500 µL of 0.5 mm diameter glass beads, conidia, germlings, and hyphae were disrupted using a FastPrep homogenizer with the following settings: 6.5 m/s, 3 times for 30 s. The samples were then centrifuged at 16,000 × g for 10 min at 4°C. The supernatants were collected and denoted “PBS extracts”. The pellets were washed twice with 1 M NaCl and another three times with 50 mM Tris-HCl, pH 7.4, followed by extraction with SDS buffer (2% (w/v) SDS, 50 mM Tris-HCl, pH 7.4, 100 mM EDTA, 150 mM NaCl and 40 mM DTT) for 10 min at 100°C. For purification of the biotinylated proteins, 1 mg of Roti®-Magbeads Streptavidin (Carl Roth, #HP57.1) were equilibrated by three washes in PBS (pH 7.4), then incubated with the protein samples for 2 h in a rotating mixer at 4°C. The beads were washed five times with four different urea buffers (buffer A, 8 M urea, 200 mM NaCl, 2% (w/v) SDS, 100 mM Tris, pH 8; buffer B, 8 M urea, 1.2 M NaCl, 0.2% (w/v) SDS, 100 mM Tris, pH 8, 10% (w/v) ethanol, 10% (w/v) isopropanol; buffer C, 8 M urea, 200 mM NaCl, 0.2% (w/v) SDS, 100 mM Tris, pH 8, 10% (v/v) ethanol, 10% (v/v) isopropanol; buffer D, 8 M urea, 100 mM Tris, pH 8) as previously described [22]. Bound proteins were isolated by incubating the streptavidin

beads with 170 µL of elution buffer (30 mM d-biotin, 8 M urea, 2% (w/v) SDS and 100 mM Tris, pH 8) for 30 min at 50°C.

2.4 Western blot analysis.

Proteins were separated by SDS-PAGE using NuPAGE 4–12% (w/v) Bis-Tris gradient gels (Thermo Fisher Scientific), and then transferred onto a PVDF membrane using the iBlot 2 dry blotting system (Thermo Fisher Scientific). To detect biotinylated proteins, 5 µg of total protein and 20 µL of purified protein were loaded, membranes were blocked with Western Blocking Reagent (Roche), and then incubated with Pierce® streptavidin-HRP (1:2,000; Thermo Fisher Scientific, #21130) overnight at 4°C. To detect the Myc-tagged proteins, 10 µg of total protein were loaded, membranes were blocked with a 5% (w/v) solution of skim milk, and then incubated with primary antibody (1:1,000; Myc-tag mouse mAb, Cell Signaling Technology, #2276) overnight at 4°C. Hybridization with a secondary antibody (HRP-linked anti-mouse IgG, Cell Signaling Technology, #7076) was performed for 1 h at room temperature. Chemiluminescence of HRP substrate was detected with the Fusion FX7 system (Vilber Lourmat, Germany).

2.5 Immunofluorescence microscopy.

The fungal materials were washed three times with PBS (pH 7.4) and then blocked with 1% (w/v) bovine serum albumin (BSA) in PBS for 1h at room temperature. For the detection of surface biotinylation, *A. fumigatus* conidia, germlings, and hyphae were incubated with Alexa Fluor™ 635 conjugated streptavidin (1:100; Thermo Fisher Scientific, S32364) for 1 h in the dark. The surface localization of Myc-tagged proteins, was examined using an anti-Myc primary antibody (1:100 of Myc-tag mouse mAb, Cell Signaling Technology, #2276) for 2 h at room

temperature and a secondary antibody (1:500; Donkey anti-mouse IgG H&L, Alexa Fluor® 568, Abcam #ab175472) for 1 h at room temperature in the dark. After three times washing with PBS, the samples were examined under a Zeiss Axio Imager M2 microscope.

2.6 In-solution protein digest with trypsin

150 µL of eluted protein samples were reduced by adding 4 µL of 500 mM TCEP (tris(2-carboxyethyl)phosphine in 100 mM TEAB) for 1 h at 55°C. 4 µL 625 mM iodoacetamide was added to each sample and incubated for 30 min at room temperature in the dark. Proteins were then precipitated using the methanol-chloroform-water method [23]. Protein samples were resolubilized in 100 µL of 100 mM triethylammonium bicarbonate (TEAB) and sonicated for 10 min. Protein content was measured with a Merck Millipore Direct Detect infrared spectrometer. The samples were treated with trypsin/Lys-C protease mix (Promega, V5072) at a protease:protein ratio of 1:25 for 16 h at 37°C. The reaction was stopped with 10 µL of 10% (v/v) formic acid and evaporated using a SpeedVac (Thermo Fisher Scientific). Peptides were resolubilized in 25 µL 0.05% (v/v) trifluoroacetic acid (TFA) and 2% (v/v) acetonitrile (ACN) in water and sonicated for 15 min in a water bath before transfer to a 10 kDa molecular weight cut-off filter. After 15 min of centrifugation at 14,000 × g (4°C), the samples were then transferred to HPLC vials and stored at -20°C.

2.7 Genetic manipulation of *A. fumigatus*.

All oligonucleotides utilized in this study are listed in Table S2. For surface localization studies, a pLJ-*Ssc70-Myc* construct was generated using pTH1 plasmid [24] as backbone. A 3,276 bp DNA fragment containing 1,010 bp 5' promoter region, the *ssc70* gene without TAA and an in-frame fused Myc-tag coding sequence was PCR amplified from genomic DNA using primers

Ssc70-M_F and Ssc70-M_R. Another 371 bp DNA fragment was amplified from pTH1 plasmid using primers Myc_F and pTH_R. These two fragments were mixed as the template and amplified using primers Ssc70-M_F and pTH_R to generate the *Ssc70-Myc* fragment. *Ssc70-Myc* fragment was digested with *Kpn*I and *Not*I, and then inserted to pTH1 plasmid using T4 ligase (Thermo Fisher Scientific) to yield the pLJ-*Ssc70-Myc* plasmid. The pLJ-*Ssc70-Myc* plasmid was then used as the backbone to generate other Myc-tag constructs. For example, a 3,073 bp DNA fragment containing *hsp70* gene and the promoter region was PCR amplified from genomic DNA using primers Hsp70-M_F and Hsp70-M_R. The DNA fragment was then inserted into the *Kpn*I and *Hin*dIII digested pLJ-*Ssc70-Myc* backbone using the CloneEZ™ PCR Cloning Kit (GenScript) to get pLJ-*Hsp70-Myc* plasmid. Primers BipA-M_F and BipA-M_R were used to amplify the *bipA* gene with promoter region. Primers Ssz-M_F and Ssz-M_R were used to amplify the *ssz* gene with promoter region. The plasmids were used to transform protoplasts from *A. fumigatus* strain A1160 (CEA17 Δ*akuB*^{KU80}) [25].

2.8 LC-MS/MS analysis.

LC-MS/MS analysis of tryptic peptides was performed on an Ultimate 3000 RSLC nano instrument coupled to a QExactive HF mass spectrometer (both Thermo Fisher Scientific). Tryptic peptides were trapped for 4 min on an Acclaim Pep Map 100 column (2 cm × 75 µm, 3 µm) at a flow-rate of 5 µL/min. The peptides were then separated on an Acclaim Pep Map column (50 cm × 75 µm, 2 µm) using a binary gradient (A: 0.1% (v/v) formic acid in H_2O; B: 0.1% (v/v) formic acid in 90:10 (v/v) ACN/H_2O): 0 min at 4% B, 6 min at 8% B, 30 min at 12% B, 75 min at 30% B, 85 min at 50% B, 90–95 min at 96% B, 95.1–120 min at 4 % B. Positively charged ions were generated by a Nanospray Flex Ion Source (Thermo Fisher Scientific) using a stainless steel emitter with 2.2 kV spray voltage. Ions were measured in data-dependent MS2

(Top15) mode: Precursor ions (z=2–5) were scanned at m/z 300–1,500 (resolution, R: 120,000 FWHM; automatic gain control, AGC target: $3 \cdot 10^6$; maximum injection time IT_{max}: 120 ms). Fragment ions generated in the HCD cell at 30% normalized collision energy using N_2 were scanned (R: 15,000 FWHM; AGC target: $2 \cdot 10^5$; max. IT: 90 ms) using a dynamic exclusion of 30 s.

2.9 Database search and data analysis of trypsin-cleaved surface peptides.

The MS/MS data were searched against the Aspergillus Genome database (AspGD) of *Aspergillus fumigatus* Af293 (http://www.aspergillusgenome.org/download/sequence/A_fumigatus_Af293/current/; 2019/02/03 YYYY/MM/DD) using Proteome Discoverer (PD) 2.2 and the algorithms of Mascot 2.4.1, Sequest HT, and MS Amanda 2.0. Two missed cleavages were allowed for tryptic peptides. The precursor mass tolerance was set to 10 ppm and the fragment mass tolerance was set to 0.02 Da. Dynamic modifications were set as oxidation (+15.995 Da) of Met and NHS-LC-Biotin (+339.162 Da) modification of Lys and the protein N-terminus. The static modification was set to carbamidomethylation (+57.021 Da) of Cys. One unique rank 1 peptide with a strict target false discovery (FDR) rate of < 1% on both peptide and protein level (compared against a reverse decoy database) were required for positive protein hits. Protein abundance quantification was performed by the Minora algorithm of PD2.2 (area under the curve approach).

2.10 Data availability

The mass spectrometry proteomics data have been deposited to the ProteomeXchange Consortium *via* the PRIDE [26] partner repository with the dataset identifier PXD018071.

3. RESULTS

3.1 Biotinylation of *A. fumigatus* surface proteins

In this study, we sought to expand the repertoire of *A. fumigatus* surface proteins and their surface-exposed epitopes, which could directly mediate pathogen-host interaction and serve as targets for diagnosis and therapy. We used the biotinylation reagent sulfosuccinimidyl-6-(biotinamido)hexanoate (Sulfo-NHS-LC-Biotin) to label the surface-exposed primary amine residues (*e.g.*, the ε-amino group of lysine residues) throughout germination of *A. fumigatus* conidia (Figure 1). The water-soluble and negatively charged Sulfo-NHS-LC-Biotin is one of the most frequently applied biotinylation reagents, particularly in regard to surface proteomics [21, 22, 27]. Samples were collected from dormant conidia grown at 37°C on AMM agar plates, swollen conidia (5 h), germlings (8 h), and hyphae (14 h) germinated at 37°C in RPMI liquid medium as described previously [11]. Although there is a possibility of biotin reagent permeation into the fungal cells [22], the biotinylation signal was confined mainly to the surface of conidia and hyphae as observed by immunofluorescence staining against biotinylated proteins (Figure 2A and Figure S1). Due to the high rigidity of the *A. fumigatus* cell wall, the fungal samples were first disrupted by glass beads in PBS buffer to release loosely attached surface proteins. This was followed by a second step using SDS buffer extraction to remove non-covalently bound hydrophobic surface proteins (Figure 1). After purification, the samples were checked by Western blot for the level of protein biotinylation and recovery from the streptavidin beads (Figure 2B and Figure S2). Proteins, varying widely in molecular mass were detected, demonstrating the ability to label a wide range of proteins using this approach. We also observed biotinylated protein bands in non-biotinylated samples (Figure 2B and Figure S2). Most likely, these represent the three known biotin-dependent carboxylases in *A. fumigatus*, encoded by Afu4g07710, Afu2g08670, and Afu5g08910, which each showed high abundance according to

the observed peptide spectrum matches (PSM) in our LC-MS/MS analyses (Dataset 1). They are easily distinguishable from the NHS-LC-Biotin modification, which adds 339 dalton of mass to the modified proteins.

Table 1. Proteins identified in all stages throughout germination in the streptavidin-enriched fractions.

Protein name	Brief description	AAs	Biotinylation sites	Detected in the samples[a]			
RodA	Conidial hydrophobin	159	K50	D	S	G	M
			K55; K126	D	S	-	-
Tef1	Putative translation elongation factor EF-1 alpha subunit	494	K472	D	S	-	M
			K476	D	S	G	-
			K483	D	S	G	M
			K486	-	-	G	-
Htb1	Histone H2B	140	K9	-	-	G	M
			K20	D	-	G	M
			K25	-	-	G	-
			K31; K134	D	S	G	M
			K60	-	-	-	M
			K99; K130	D	-	-	-
			K100	D	-	-	M
Afu5g10550	ATP synthase F1, beta subunit	519	K122	D	S	G	M
			K148	-	S	G	-
			K151	-	S	-	-
			K338; K392; K473	-	-	G	-
Bgt1	1,3-beta-glucanosyltransferase	305	K36	-	-	G	-
			K51; K69; K145; K275	-	S	-	-
			K125; K141; K304	D	S	G	M
Afu3g00880	Putative adhesin protein	219	K24	D	S	G	M
			K63		S	G	M

DppV	Secreted dipeptidyl-peptidase	721	K136; K351; K373; K423	-	-	-	M
			K239; K328	-	-	G	M
			K327	-	S	G	M
			K702	D	-	G	-
Bgt2	Cell wall glucanase	446	K139; K231	-	-	-	M
			K225	D	S	G	M
GldB	Putative glycerol dehydrogenase	325	K268	D	S	G	M
			K297	D	S	-	-
ArtA	14-3-3 family protein	261	N-term	D	S	G	M
Afu2g02100	Putative dihydrolipoamide dehydrogenase	513	K204; K269; K383	-	-	G	-
			K273; K283; K302; K351	-	-	-	M
			K286; K420	-	-	G	M
			K435	D	S	G	M
Afu3g05360	Has domain(s) with predicted DNA binding, protein heterodimerization activity	265	K9; K76; K77	-	-	-	M
			K14	D	-	G	M
			K22	D	S	-	M
			K38	D	-	-	M
Afu4g10410	Putative aspartate aminotransferase	429	K72	-	-	G	M
			K85	D	S	-	-
Afu5g13450	Putative triosephosphate isomerase	249	K102	-	S	-	-
			K137	D	-	-	-
			K216	-	-	G	M
Afu1g16523	Ortholog(s) have structural constituent of ribosome activity and cytosolic small ribosomal subunit localization	93	K37	D	S	G	M

[a] the lysine residues of the protein detected with biotinylation in dormant (D), swollen (S), germinating (G) conidia, hyphae (M) and not detected (-) are indicated.

3.2 Identification of constitutively, and stage-specifically, exposed proteins

LC-MS/MS analysis resulted in a proteome set consisting of 1139 different *A. fumigatus* proteins, which were detected with at least 2 peptides and/or a PSM value ≥ 10. Approximately 28% (314) of the detected proteins had a detectable NHS-LC-Biotin modification when

considering all germination conditions (Figure 3A). 77 proteins had a predicted signal peptide and 22 proteins had at least one transmembrane domain (fungidb.org; [28]). Over the course of germination, 74 proteins with biotinylation were identified on dormant conidia, 75 on swollen conidia, 93 on germlings, and 214 on hyphae. Most of the proteins detected with biotin modifications were found in PBS extracts, only a few (5 to 14) were exclusively found in SDS extracts (Figure 3A, 3B, and Dataset 1). In accordance with our previous surface proteomics study based on a trypsin-shaving approach [11], our data confirm the dynamic change of the surface-exposed proteome of *A. fumigatus* across germination. There were 24, 16, 30, and 146 proteins detected exclusively on dormant, swollen, germinating conidia, and hyphae, respectively (Figure 3C).

Throughout germination, 15 proteins were biotinylated in all four stages (Table 1), including several already described surface proteins, for example, RodA [12], the translational elongation factor 1 alpha Tef1 [29], the peptidase DppV [30], the 1,3-beta-glucanosyltransferase Bgt1[31] and Bgt2 [32], the 14-3-3 protein ArtA [29], and the MedA-regulated, putative adhesin Afu3g00880 [33]. The biotinylation of RodA K50 was detected in all four stages, while the biotinylation of K55 and K126 was only detected in dormant and swollen conidia (Table 1). All lysine residues are localized in α-helical regions of the protein [9]. RodA also exhibited high abundance in conidia but not mycelium (Table 2 for top 15). Tef1 was detected mainly in SDS extracts (Table S3). The biotinylation of Tef1 was detected at sites K472, K476, K483, and K486, indicating that the C-terminus of Tef1 was exposed on the conidial and mycelial surface. Somewhat surprisingly, the histone H2B (Htb1, Afu3g05350) seemed to be one of the most abundant proteins throughout the germination course (Table 1 and 2). The total PSM value of Htb1 in dormant conidia was even higher than that of RodA (Dataset 1) in contrast to previous

297 studies using different approaches [10]. One possible explanation for this difference is the
298 difference in the total number of the modifiable lysines in each protein. There are 23 lysine
299 residues in the 140 amino acid residues (AAs) of Htb1, 9 of which were detected with a
300 biotinylation modification (Table 1). In contrast, there are only 9 lysine residues present in the
301 hydrophobic protein RodA.

302 **Table 2**. LC-MS/MS analysis of highly abundant proteins detected throughout the germination
303 course (top 15 of each morphotype).

Protein	Protein Description	AAs	Top 15 in developmental stages	Biotinylation sites[a]
Htb1[b]	Histone H2B	140	D, S, G, M	Table 1
RodA[b]	Conidial hydrophobin	159	D, S, G	Table 1
Afu5g10550[b]	ATP synthase F1, beta subunit	519	D, S, G	Table 1
UbiA*	Ubiquitin	128	D, S	K6[s]; K33[d, s]; K48[d, s]
UbiC*	Ubiquitin (Afu3g11260), putative	154	D, S	K6[s]; K11[s]; K33[d, s]; K48[d, s]
Tef1[b]	Translation elongation factor EF-1 alpha subunit	494	D, S	Table 1
Sod1[b]	Cu/Zn superoxide dismutase	154	D, S	K43[d, s, g]
GpdA[b]	Glyceraldehyde-3-phosphate dehydrogenase	338	D, S	K194[d, m]; K215[d, s, m]
Pil1	Cell wall integrity signaling protein	345	D, S	K29[d]; K45[d, s]; K131[d, s]; K160[d, s]; K270[d]
Afu7g01060	Cysteine-rich secreted protein	343	D, S	K212[d, s]; K224[d, s]
Afu2g13860	Histone H4	142	D	K71[d, m]; K117[m]
Ecm33	GPI-anchored cell wall organization protein	398	D	K170[s, m]; K306[d]; K334[m]
Scf1[b]	Putative heat shock protein	89	D	K81[d]
Grg1[b]	Glucose-repressible gene	69	D	K28 or K32[s]; K32[d]; K46[d, s]
ConJ[b]	Conidiation-specific protein	83	D	N-Term[d]; K48[d]
CatA	Spore-specific catalase	750	D	K534[d]; K534 or K537[s]; K537[d]; K608 or K612[s]
CpcB	G-protein complex beta subunit	316	S, G	K38[g]; K56[d, s, g]; K172[g]; K277[s, g]
Asp f MDH[b]	Putative NAD-dependent malate dehydrogenase	340	S, G	K91[g]; K185 or K186[m]; K238[s, g, m]; K263[s, g, m]; K269[g]; K303[g]; K309[g, m]; K327[m]; K331[m]
Afu8g05320[b]	Putative mitochondrial F1 ATPase subunit alpha	556	S, G	K135s; K164g; K170g, m; K170 or K172s; K233g; K243g; K427g, m; K430g; K531g

Afu1g04070	Eukaryotic initiation factor 5A	157	S	K40[s]; K69[s]
RodB	Conidial cell wall hydrophobin	183	S	K105[s]
Bgt1	Putative 1,3-beta-glucanosyltransferase	305	S	Table 1
Afu3g00880	Putative adhesin protein	219	G, M	Table 1
Afu4g07710	Putative pyruvate carboxylase	1193	G, M	K571[m]; K684[m]; K1004[m]; K1157[g]
Afu6g13250[b]	60S ribosomal protein L31e	123	G, M	K30[m]; K59[m]; K69[m]; K70[g]; K111[g]
Sod3/Asp f 6	Manganese superoxide dismutase	210	G	K50[g]; K59[g]; K88[g, m]; K93[g, m]; K101[g]; K202[m]
Hsp70[b]	Heat shock protein	638	G	K54[m]; K185[g]; K244[m]; K249[g, m]; K421[g]; K449[m]; K498[g, m]; K505[g, m]; K510[g, m]; K522[g]; K555[m]
PgkA[b]	Putative phosphoglycerate kinase	417	G	K32[g]; K33[g]; K79[g]; K246[g]; K264[g]
Afu3g12300	60S ribosomal protein L22	124	G	K17[g]
Afu4g04460	60S ribosomal protein L13	226	G	K225[g]; K226[d]
Ndk1	Putative nucleoside diphosphate kinase	153	G	K84[g, m]
Asp f 4	Allergen Asp f 4	322	M	K140[s, m]; K155 or 156[m]; K220[m]; K306[m]
Afu2g09200	60S ribosomal protein L30	106	M	K34[m]
Afu1g11130	60S ribosomal protein L6	200	M	K107[m]
Afu1g05390	ATP:ADP antiporter activity	308	M	K103[m]; K146[g, m]; K149[m]; K252[m]; K264[m]
Afu3g06840	Cytosolic small ribosomal subunit S4	261	M	K106[m]
Afu3g06960	60S ribosomal protein L21	158	M	K20[m]; K107[m]; K110[m]
GliT	Gliotoxin sulfhydryl oxidase	334	M	K117[m]; K227[m]
Gel2/Asp f GT	GPI-anchored 1,3-beta-glucanosyltransferase	475	M	K36[m]; K187[m]; K372[m]; K379[s, m]; K388[m]; K393[m]
Afu6g12990[b]	Cytosolic large ribosomal subunit protein L7A	263	M	K8[m]; K212[m]; K229[m]; K255[s]
BtgE	Putative cell wall glucanase	616	M	K376[m]; K387[m]; K389[m]; K577[g, m]
Afu4g07730	60S ribosomal protein L11	176	M	K79[m]; K91[m]; K157[m]

[a] Lysine residues of the protein detected with biotinylation marks in dormant ([d]), swollen ([s]), germinating ([g]) conidia and hyphae ([m]) are indicated. [b] Proteins commonly detected in different surface proteomics data, see also Table S3.

* have shared peptides mapped to different proteins.

3.3 Immunoreactive proteins are exposed on the surface of *A. fumigatus*

In a unique subset of atopic individuals, sensitization to *A. fumigatus* allergens can develop into allergic asthma, allergic sinusitis, and following fungal lung colonization into ABPA [2]. Twenty-three different allergens have been reported in accordance to the systematic allergen

311 nomenclature (www.allergome.org), but actually more than 100 immunoreactive *A. fumigatus*
312 proteins have already been detected by immunoproteomic studies [5]. In our work, 22 allergens
313 (Table 3) were detected by surface biotinylation. The allergens Asp f 17, Asp f 18, Asp f 27, Asp
314 f Mannosidase, Asp f Catalase, and Asp f Glucosidase were detected on dormant conidia. The
315 biotinylation of Asp f 27 K140 was detected on dormant, swollen, and germinating conidia. In
316 addition to Asp f 27, three allergens (Asp f 9, Asp f FDH, and Asp f MDH) were detected on
317 swollen conidia, germlings, and hyphae. Biotinylation of Asp f 9 K190, Asp f MDH K238, and
318 K263 were detected on the three different morphologies of *A. fumigatus*. Ten allergens were only
319 detected on germlings and/or hyphae (Table 3). Consistent with the literature, these data again
320 clearly demonstrate that numerous known *A. fumigatus* allergens are exposed on the fungal
321 surface [9-11, 18, 34].

322 In addition to the allergens, there were also other immunoreactive proteins that could
323 serve as biomarkers for diagnosis or targets for allergen immunotherapy [35-37]. DppV, Bgt1,
324 Bgt2, and Afu5g10550 were detected with biotinylation modifications in all four morphotypes
325 (Table 1). Afu5g10550 encodes an ATP synthase F1 beta subunit, which reacts with immunosera
326 from rabbits exposed to *A. fumigatus* conidia [35]. Biotinylation of Afu5g10550 K122 was
327 detected throughout germination. It was also one of the most prevalent proteins detected on
328 dormant, swollen, and germinating conidia (Table 1 and 2). The immunoreactive GpdA, Asp f
329 MDH, Bgt1, Asp f 6, PgkA, Asp f 4, GliT, Asp f GT, and Hsp70 were also prevalent on the
330 surface of one or two morphological stages (Table 2).

331 **Table 3**. *A. fumigatus* allergens exposed to the surface.

Allergen[a]	Protein Description	AAs	Detected in the samples	Biotinylation sites

Asp f 1	Mitogillin	176	G, M	K96[g, m]; K138[g]; K140[g]
Asp f 2	Allergen Asp f 2	314	M	K83[m]
Asp f 4	Allergen Asp f 4	322	S, M	K140[s, m]; K155 or 156[m]; K220[m]; K306[m]
Asp f 6 (Sod3)	Putative manganese superoxide dismutase	210	G, M	K50[g]; K59[g]; K88[g, m]; K93[g, m]; K101[g]; K202[m]
Asp f 9	Cell wall glucanase	395	S, G, M	K190[s, g, m]
Asp f 11 (Cyp4)	Putative cyclophilin	205	S	K119[s]
Asp f 12 (Hsp90)	Heat shock protein	706	G	K481[g]
Asp f 17 (Mp1)[b]	Putative cell wall galactomannoprotein	284	D	K63[d]; K144[d]
Asp f 18 (Alp2)	Autophagic (vacuolar) serine protease	495	D	K261[d]; K268[d]; K271[d]; K291[d]
Asp f 23 (RpL3)	Allergenic ribosomal L3 protein	392	M	K5[m]
Asp f 27[b]	Putative peptidyl-prolyl cis-trans isomerase	163	D, S, G	K43[d, s]; K140[d, s, g]; K152 or K153[d]
Asp f 28[b]	Putative thioredoxin	171	M	K125[m]
Asp f Mannosidase (MsdS)[b]	Putative 1,2-alpha-mannosidase	503	D	K212[d]; K274[d]; K415[d]; K416[d]; K488[d]
Asp f Catalase (Cat1)[b]	Catalase	728	D	K261[d]; K346[d]; K466[d]
Asp f Glucosidase (Exg12)[b]	Secreted beta-glucosidase	863	D, M	K127[d]; K178[d]; K415[d]; K603[d]; K839[d]; K843[d, m]
Asp f FDH	Putative NAD-dependent formate dehydrogenase	418	S, G, M	K304[m]; K319[s, g]; K327[m]
Asp f MDH[b]	Putative NAD-dependent malate dehydrogenase	340	S, G, M	K91[g]; K185 or K186[m]; K238[s, g, m]; K263[s, g, m]; K269[g]; K303[g]; K309[g, m]; K327[m]; K331[m]
Asp f GT (Gel2)	GPI-anchored 1,3-beta-glucanosyltransferase	475	S, M	K36[m]; K187[m]; K372[m]; K379[s, m]; K388[m]; K393[m]
Asp f GPI	Putative glucose-6-phosphate isomerase	553	M	K35[m]; K451[m]
Asp f AT_V	Putative class V aminotransferase	386	M	K381[m]
Asp f gamma_Actin (Act1)[b]	Actin	393	M	K346[m]
Asp f RPS3[b]	40S ribosomal protein S3	266	M	K78[m]

[a] *A. fumigatus* allergens based on allergome website (www.allergome.org). [b] Allergens commonly detected in different surface proteomics data, see also Table S3.

3.4 Heat shock proteins are exposed to the surface

Heat shock proteins (HSPs) and a large set of co-chaperones are ubiquitous molecular chaperones that act in maintaining protein homeostasis [38]. It has been well established that HSPs are also secreted extracellularly or localized on the cell surface [39]. Hsp90, also known as

Asp f 12, is detectable on the cell wall of *A. fumigatus* [34] and it was also found to be biotinylated in this study (Table 3). Considering the detection of biotinylated Hsp90 and Hsp70, we investigated whether other chaperone-related proteins are present on the cell surface of *A. fumigatus*. Indeed, at least 16 chaperone-related proteins were detected with biotinylation modifications (Table 4). Most of the chaperones were detected on the surface of germlings or hyphae with the exception of Scf1 and GrpE. Scf1 shows similarities to the 12 kDa heat shock protein of *S. cerevisiae* and was biotinylated at K81 (Table 4). It is one of the most prevalent proteins on dormant conidia of the *A. fumigatus* strains CEA10 (Table 2) and ATCC 46645 [10]. Six chaperones (Hsp70, Hsp88, HscA, BipA, Ssc70, and Lhs1) belonging to the Hsp70 family were detected in our study (Table 4). In addition to Hsp70, four other Hsp70 family proteins (Sti1, Hsp88, HscA, and Ssc70) have shown to induce serological antibody responses in ABPA patients [37].

Table 4. Chaperones and co-chaperones with cell surface localization.

Protein	Accession	Protein Description	AAs	Detected in the samples	Biotinylation sites
Scf1	Afu1g17370	Putative heat shock protein	89	D	K81
GrpE	Afu2g13040	Mitochondrial co-chaperone	250	D, S	K99[d, s]
Wos2	Afu5g13920	Putative Hsp90 binding co-chaperone	201	S, G	K35[g]; K193[s]
Hsp60	Afu2g09290	Putative antigenic mitochondrial protein	587	G	K510
Hsp90/Asp f 12	Afu5g04170	Heat shock protein	706	G	K481
Afu6g10700	Afu6g10700	Ortholog(s) have chaperone binding, unfolded protein binding activity	122	G	K50; K56
Sti1	Afu7g01860	Putative heat shock protein	581	G	K232
Hsp70	Afu1g07440	Molecular chaperone	638	G, M	Table 2
Hsp88	Afu1g12610	Hsp70 chaperone	714	G, M	K130 or K133[m]; K216[m]; K260[m]; K271[g, m]
HscA	Afu8g03930	Putative Hsp70 chaperone	614	G, M	K59[m]; K429[g]; K498[g]; K531[g]; K539[g]; K566 or K568[g]; K609[g]

BipA	Afu2g04620	Hsp70 chaperone	672	G, M	K133[m]; K549[g, m]
Ssc70	Afu2g09960	Putative mitochondrial Hsp70 chaperone	661	G, M	K92[g, m]; K113[m]; K124[g, m]; K192[g]; K277[m]; K278[m]; K453[g]
Lhs1	Afu1g15050	Hsp70 family chaperone	997	M	K341
ClxA	Afu4g12850	Calnexin, ER membrane chaperone	563	M	K153
Egd2	Afu6g03820	Nascent polypeptide-associated complex subunit alpha	204	M	K50; K51; K62
Afu6g10320	Afu6g10320	Unfolded protein binding activity	496	M	K143

To confirm the surface localization of the HSPs, we generated constructs by fusing a Myc-tag to the C-terminus of the HSPs. These constructs were ectopically integrated into the genome of *A. fumigatus* (Supplementary Table 1 and 2). The *hsp70-Myc*, *ssc70-Myc*, *bipA-Myc* and *ssz-Myc* transformants were verified by immunoblotting using an anti-Myc tag antibody (Figure S3). Using immunofluorescence microscopy, we found that all of the Myc-tagged fusion proteins were localized on the surface (Figure 4), except for the negative control, the HSP 70 chaperone Ssz (Afu2g02320), which was not detected on the surface in our biotinylation experiment. This independently confirms that HSPs of *A. fumigatus* are localized to the cell surface of the fungus.

3.5 The core surface proteome (surfome) of *A. fumigatus*

Considering that several surface proteomic studies have been performed using different methods (trypsin-shaving, HF/pyridine, and formic acid extraction), we attempted to compare these datasets to provide a more comprehensive picture of the *A. fumigatus* surfome [9-11]. In total, 992 different proteins were detected as surface proteins in this study and the aforementioned studies, including 437 proteins that were detected by at least two approaches (Figure 5 and Table S3). 43 proteins were commonly identified in all studies (Figure 5 and Table S3). These 43

proteins include 15 of the most prevalent proteins identified in our study and 9 allergens (Table 2, 3, and S3). Two small proteins, Grg1 (glucose-repressible gene) and ConJ (conidiation-specific protein 10), were both detected among the most prevalent proteins on dormant conidia of the ATCC 46645 strain using the HF-pyridine extraction method [10], on the CEA10 strain using the trypsin shaving method [11], and in this study using biotinylation (Table 2). Grg1 was detected with biotinylation at the positions K32 and K46, while ConJ was biotinylated at the N-terminus and site K48 (Table 2). The conidial surface protein CcpA, which contributes to fungal virulence, was detected with biotinylations at positions K41 and K90 (Table S3). The putative GPI-anchored cell wall protein CweA [11] was detected with a biotinylation marker at site K358 (Table S3). In addition to the 43 commonly detected proteins, 68 proteins were detected in at least four surfome datasets (Figure 5A), 44 of which were detected with biotinylated amino-groups (Table S3), including five allergens (Asp f 1, Asp f 4, Asp f 11, Asp f 12, and Asp f 18) and seven other prevalent proteins (1,3-beta-glucanosyltransferase Bgt1, cell wall protein Ecm33, nucleoside kinase Ndk1, eukaryotic initiation factor 5A [Afu1g04070], a putative ADP/ATP carrier [Afu1g05390], the 60S ribosomal protein L13 [Afu4g04460], and ubiquitin [Afu3g11260]) (Table 2). In total 133 surface proteins with biotinylation modifications were also confirmed by alternative methods (Figure 5B). All in all, the core-surfome of *A. fumigatus* builds a valuable database to provide protein targets for further studies on host-pathogen interactions, diagnosis, and immunotherapy.

4. DISCUSSION

Proteins in combination with other cell wall components on the surface of *A. fumigatus* conidia play a key role in protecting the fungus from environmental insults and host defense responses

during an infection [10, 12, 15, 40, 41]. Several methods and techniques have been used to investigate the surface proteins of this pathogenic fungus, leading to the detection of hundreds of surface proteins, whose presence on the surface changes dynamically during development [9-11, 19, 42]. Most methods used for the extraction of surface proteins, like enzymatic treatment with glucanase or trypsin or acidic extraction with formic acid or hydrogen-fluoride–pyridine, have the potential to release intracellular, unexposed cell wall proteins. Cell impermeable biotinylation reagents, which react with primary amines accessible on the cell surface, have successfully been used for labeling and identification of surface proteins with little contamination [15, 21, 22, 43, 44]. To further expand the *A. fumigatus* surface proteome and to solidify the data of the common core surfome of *A. fumigatus*, we used a surface biotinylation approach, which has not been applied to *A. fumigatus* previously. The aim was to characterize and detail the *A. fumigatus* surfome with surface exposed regions across germination and verify the surface localization of selected proteins by an additional method (Figure 4). Therefore, our work provides a multitude of candidates for further investigation of host-pathogen interaction and possible immuno-diagnostic/therapeutic usages.

Proteins on the surface mediate the direct contacts between pathogens and hosts. In addition to several known surface proteins, like RodA, CalA, Asp f 2, and CcpA [10, 12, 15, 18], abundant surface proteins detected in this study, such as Tef1, ArtA, Hsp70 and Hsp90, also have the potential to interact with a range of host proteins [45]. The *Candida albicans* Tef1 was shown to be able to bind human plasminogen, probably through the C-terminal lysine residues [46]. In this study, Tef1 was detected with biotinylation at the C-terminal K472–K486 region throughout germination (Table 1), indicating that Tef1 in *A. fumigatus* might have a similar function. The 14-3-3 proteins, such as ArtA, also have the ability to bind a multitude of proteins,

and play an important role in morphogenesis and sensing of environmental cues in fungi [47-49]. The surface-localized heat shock proteins influence the interaction between bacterial and fungal pathogens and host cells as well [50-52]. For example, expression of *Listeria monocytogenes* heat shock protein ClpC, a member of the 100-kDa heat shock protein family, is required for cell adhesion and invasion [53], and also allows this bacterium to escape from the phagosome [54]. The *C. albicans* Hsp70 protein Ssa1 is an invasin that binds to host cell cadherins to induce host cell endocytosis, which is critical for *C. albicans* to cause maximal damage [55]. In line with this, the *A. fumigatus* Hsp70 and Hsp90 were predicted to interact with host proteins in conidia containing mouse macrophage phagolysosomes [45], suggesting the potential roles of surface heat shock proteins in manipulating the host immune responses.

Besides their roles in pathogenicity, surface proteins could also be targets of immunotherapies based on antibodies. Surface proteins are particularly suitable due to their easy accessibility. Antibody-based therapies are rapidly growing, since they are a promising approach to directly attack the pathogen and boost the innate immune system. However, only a few monoclonal antibodies against fungal pathogens have been developed and advanced to clinical trials [56]. One example is Mycograb, an Hsp90-specific antibody fragment, which showed promise for treating *Candida* infections in combination with amphotericin B [57], but failed to obtain marketing authorization. In mouse experiments, treatment with anti-HSP 60 antibodies reduced fungal burden after infection with the dimorphic fungi *Histoplasma capsulatum* and *Paracoccidioides lutzii* [58, 59]. On the negative side, the amino acid sequences of HSPs are highly conserved and cross-reactivity may occur. For example, the epitope (NKILKVIRKNIVKK) that Mycograb targets shows high similarity between yeast, mice, and human homologues of Hsp90 [57], including *A. fumigatus* Hsp90 (NKIMKVIKKNIVKK, amino

436 acids 383–396). Other, abundant, fungal-specific surface proteins may represent better targets for
437 immunotherapy as discussed in the following.

438 To date, more than 100 antigens or immune-reactive proteins of *A. fumigatus* have been
439 identified using classical immunobiological procedures that react with sera from ABPA patients
440 or animal models [35-37]. However, only a few recombinant allergens have been used
441 commercially for diagnosis of allergic aspergillosis [5]. Although the crystal structures of some
442 allergens are known [60, 61], the question of whether the allergen/protein exhibits special
443 structural characteristics that are responsible for its allergenicity is still poorly understood. Thus,
444 the information about the association of allergens with the different morphotypes (conidia,
445 mycelium) and their exposed regions that may directly mediate the interaction with host
446 components, such as IgE binding, is needed. Such knowledge creates the basis for the
447 understanding of the immunological properties of protein antigens and is important for the
448 establishment of new forms of diagnosis and treatment [62].

449 The cyclophilins, including Asp f 11 and Asp f 27 [61], which are structurally conserved
450 pan-allergens showing extensive cross-reactivity [63, 64]. It was reported that the conserved
451 N81–N149 region of Rhi o 2 from *Rhizopus oryzae* (Figure S4) is crucial for IgE-recognition and
452 cross-reactivity [63]. In this study, however, the C-terminal region of Asp f 27, which is not
453 conserved, was detected with biotinylation marks instead (Table 3 and Figure S4). Several other
454 allergens were detected with biotinylation sites on different morphotypes, such as the K50–K101
455 region of Asp f 6, K304–K327 region of Asp f FDH, K238–K269, and K303–K331 region of
456 Asp f MDH (Table 3). Noteworthy, there were also regions of surface proteins that were detected
457 on all morphotypes. For example, the K50–K55 region of RodA, K472–K486 region of Tef1,
458 K122 region of Afu5g10550, K125–K141 region of Bgt1, K24–K63 region of Afu3g00880,

K225–K231 region of Bgt2, and K420–K435 region of the putative dihydrolipoamide dehydrogenase Afu2g02100 were all consistently surface exposed (Table 1). These peptides may represent promising candidate antigens for the development of monoclonal antibodies to be used for diagnosis and immunotherapy.

As published in our previous study, the surfome of *A. fumigatus* is dynamic [11]. Correspondingly, a recent study also revealed that the phenotypes of *A. fumigatus* germinating conidia vary among genetically identical conidia. Here, we detected 74, 75, and 93 proteins on dormant, swollen, and germinating conidia, respectively; while 214 proteins were found on the surface of hyphae (Figure 3). Comparison of the different surface proteomics datasets helped to identify the core-surfome of *A. fumigatus* (Figure 5). These proteins, which are consistently found on the surface of *A. fumigatus*, likely play a role in mediating the interaction of *A. fumigatus* with the host or other organisms.

5. CONCLUSION

A surface biotinylation enrichment coupled with LC-MS/MS analysis was applied to study the surface proteome of *A. fumigatus* across germination. 314 surface proteins, including RodA, some virulence factors, allergens, and newly identified surface proteins were detected with biotinylation modifications, confirming exposed surfaces for these proteins. These data highlight not only the surface proteins but also the exposed regions that could be used in the future for new diagnostic tools and immunotherapies based on monoclonal antibodies or T cell-based vaccines.

ASSOCIATED CONTENT

Supporting Information

Table S1. *A. fumigatus* strains used in this study.

Table S2. Oligonucleotides used in this study.

Table S3. Proteins of *A. fumigatus* detected with biotinylation marks.

Dataset 1. Streptavidin enriched *A. fumigatus* proteins detected by LC-MS/MS. For the headers, B1, B2, B3, and B4 are different repeats of biotinylated samples; C1, C2, C3, and C4 are different repeats of control samples.

Figure S1. Immunofluorescence staining of biotinylated (A) and non-biotinylated (B) *A. fumigatus* morphotypes with Alexa Fluor™ 635 conjugated streptavidin (Streptavidin-AF635). Germlings indicated with dashed boxes are also shown in Figure 2A. Scale bar is 10 μm.

Figure S2. Immunoblotting analysis of swollen conidia and mycelia protein extracts. Crude protein extracts (crude) and purified proteins (streptavidin purified) from PBS buffer (PBS) and SDS buffer (SDS) were separated on SDS-PAGE and then transferred to PVDF membrane. Biotinylated proteins were detected with Pierce® streptavidin-HRP. B, biotinylated; N, non-biotinylated.

Figure S3. Immunoblotting of *A. fumigatus* protein extracts. Myc-tagged proteins were detected using α-Myc antibody. For the *hsp70-Myc* and *ssc70-Myc* expressing *A. fumigatus* strains, protein was extracted from dormant conidia; while for the *ssz-Myc* and *bipA-Myc* expressing strains, protein was extracted from mycelium. An α-GAPDH antibody served as loading control.

Figure S4. Alignment of Asp f 27 and homologous proteins. Lysine residues of Asp f 27 detected with biotinylation marks in this study are indicated with arrows. Protein sequences of Asp f 27 (UniProtKB: Q4WWX5), CaCYP1 (*Candida albicans*, UniProtKB: P22011), and CPR1 (*Saccharomyces cerevisiae*, UniProtKB: P14832), and Rhi o 2 (*Rhizopus delemar*, UniProtKB: P0C1H7) are downloaded from UniProt Knowledgebase (www.uniprot.org). Protein sequences

of Ole e 15 (*Olea europaea*, GenBank: AVV30163.1), HuCYPA (Homo sapiens, GenBank: AAH05982.1), and ROC5 (*Arabidopsis thaliana*, NCBI Reference Sequence: NP_195213.1) were downloaded from NCBI (www.ncbi.nlm.nih.gov).

AUTHOR INFORMATION

Corresponding Author

*Email: olaf.kniemeyer@leibniz-hki.de (OK); axel.brakhage@leibniz-hki.de (AAB);

Tel: 49 (0)3641-532 1071 (OK); 49 (0)3641-532 1001 (AAB).

ORCID

Lei-Jie Jia: 0000-0001-7958-6187;

Thomas Krüger: 0000-0001-8984-3853

Matthew G. Blango: 0000-0001-8015-9019;

Olaf Kniemeyer: 0000-0002-9493-6402;

Axel A. Brakhage: 0000-0002-8814-4193.

Notes

The authors declare no conflicts of interest.

ACKNOWLEDGMENT

This work was supported by the Deutsche Forschungsgemeinschaft (DFG)-funded French-German project “AfuInf”, the DFG Collaborative Research Center/Transregio FungiNet 124 ‘Pathogenic fungi and their human host: Networks of Interaction’ (project A1, Z2), and the

Federal Ministry of Education and Research, project EXASENS (13N13861). The funder had no role in the design or choice to publish these data.

Figure legends

Figure 1. Flowchart for the biotinylation and purification of *A. fumigatus* surface proteins. The procedure starts with covalent labeling of surface proteins with Sulfo-NHS-LC-Biotin for 30 min at 4°C. The fungal material was broken with glass beads in PBS buffer to release the loosely attached surface proteins (PBS extracts). Some non-covalently linked cell wall proteins were extracted using SDS buffer. Biotinylated proteins were purified using magnetic streptavidin beads and then analyzed by LC-MS/MS.

Figure 2. Detection of *A. fumigatus* surface protein biotinylation. (A) Immunofluorescence staining of *A. fumigatus* dormant conidia and germinating conidia with Alexa Fluor™ 635 conjugated streptavidin (Streptavidin-AF635). Scale bar is 10 μm. (B) Immunoblotting analysis of the crude protein extracts and purified proteins from dormant and germinating conidia. B, biotinylated; N, non-biotinylated; PBS, PBS extracts; SDS, SDS buffer extracts; CBB, Coomassie brilliant blue.

Figure 3. Overview of the surface proteome identified by biotinylation coupled with LC-MS/MS analysis. (A) Number of proteins identified in different samples. [a], number of proteins identified by at least two unique peptides or with PSMs (peptide spectrum matches) ≥ 10 were considered. [b], number of proteins detected with at least one peptide with biotinylation modification. (B and C) Venn diagrams showing the common and specific surface proteins with biotinylation across different extractions (B) and developmental stages (C).

Figure 4. Immunofluorescence staining of *A. fumigatus* germlings. Germlings were blocked in PBS with 1% (w/v) BSA, and then incubated with the primary anti-Myc antibody. The surface Myc-tagged Hsp70s were indirectly detected with an AF568 conjugated secondary antibody. Scale bar = 10 μm.

Figure 5. The number of *A. fumigatus* surface proteins identified in different surface proteomics experiments. (A) Pie chart shows the number of proteins present in different experiments. (B) Each of the bars represents the number of identified proteins, with black zones highlighting the number of proteins present in all of the surfome data available, including the results obtained in this study (CEA10 B, CEA10 using biotinylation method), the surfome of CEA10 (CEA10 T, CEA10 using trypsin shaving method) and D141 obtained using trypsin shaving method [10, 11], the CEA17Δ*akuB*^{KU80} dormant conidia surfome obtained from the formic acid extract [9], and the ATCC 46645 surfome detected by hydrogen fluoride-pyridine extraction and trypsin shaving [10]. The pink zones highlight the number of proteins present in at least two but not all the surfome data. Grey zones indicate the number of proteins present in just one experiment.

REFERENCES

[1] C. Kosmidis, D.W. Denning, The clinical spectrum of pulmonary aspergillosis, Thorax 70(3) (2015) 270-7.
[2] J.P. Latgé, G. Chamilos, *Aspergillus fumigatus* and Aspergillosis in 2019, Clin. Microbiol. Rev. 33(1) (2019) e00140-18.
[3] R. Agarwal, A. Chakrabarti, A. Shah, D. Gupta, J.F. Meis, R. Guleria, R. Moss, D.W. Denning, A.c.a.I.w. group, Allergic bronchopulmonary aspergillosis: review of literature and proposal of new diagnostic and classification criteria, Clin. Exp. Allergy 43(8) (2013) 850–873.
[4] M. Kousha, R. Tadi, A.O. Soubani, Pulmonary aspergillosis: a clinical review, Eur. Respir. Rev. 20(121) (2011) 156–174.
[5] B. Singh, S. Singh, A.R. Asif, M. Oellerich, G.L. Sharma, Allergic aspergillosis and the antigens of *Aspergillus fumigatus*, Curr. Protein Pept. Sci. 15(5) (2014) 403–423.
[6] S.M. Levitz, *Aspergillus* vaccines: Hardly worth studying or worthy of hard study?, Med. Mycol. 55(1) (2017) 103–108.

[7] O. Kniemeyer, F. Ebel, T. Kruger, P. Bacher, A. Scheffold, T. Luo, M. Strassburger, A.A. Brakhage, Immunoproteomics of Aspergillus for the development of biomarkers and immunotherapies, Proteomics Clin Appl 10(9-10) (2016) 910-921.
[8] M.G. Blango, O. Kniemeyer, A.A. Brakhage, Conidial surface proteins at the interface of fungal infections, PLoS Pathog. 15(9) (2019) e1007939.
[9] I. Valsecchi, V. Dupres, J.P. Michel, M. Duchateau, M. Matondo, G. Chamilos, C. Saveanu, J.I. Guijarro, V. Aimanianda, F. Lafont, J.P. Latgé, A. Beauvais, The puzzling construction of the conidial outer layer of *Aspergillus fumigatus*, Cell. Microbiol. 21(5) (2019) e12994.
[10] V. Voltersen, M.G. Blango, S. Herrmann, F. Schmidt, T. Heinekamp, M. Strassburger, T. Kru□ger, P. Bacher, J. Lother, E. Weiss, K. Hu□nniger, H. Liu, P. Hortschansky, A. Scheffold, J. Lo□ffler, S. Krappmann, S. Nietzsche, O. Kurzai, H. Einsele, O. Kniemeyer, S.G. Filler, U. Reichard, A.A. Brakhage, Proteome analysis reveals the conidial surface protein CcpA essential for virulence of the pathogenic fungus *Aspergillus fumigatus*, MBio 9(5) (2018) e01557-18.
[11] M.G. Blango, A. Pschibul, F. Rivieccio, T. Krüger, M. Rafiq, L.-J. Jia, T. Zheng, M. Goldmann, V. Voltersen, J. Li, G. Panagiotou, O. Kniemeyer, A.A. Brakhage, The dynamic surface proteomes of allergenic fungal conidia, J. Proteome Res. (2020).
[12] V. Aimanianda, J. Bayry, S. Bozza, O. Kniemeyer, K. Perruccio, S.R. Elluru, C. Clavaud, S. Paris, A.A. Brakhage, S.V. Kaveri, L. Romani, J.P. Latgé, Surface hydrophobin prevents immune recognition of airborne fungal spores, Nature 460(7259) (2009) 1117–1121.
[13] J. Carrion Sde, S.M. Leal, Jr., M.A. Ghannoum, V. Aimanianda, J.P. Latgé, E. Pearlman, The RodA hydrophobin on *Aspergillus fumigatus* spores masks dectin-1- and dectin-2-dependent responses and enhances fungal survival in vivo, J. Immunol. 191(5) (2013) 2581–2588.
[14] N. Thau, M. Monod, B. Crestani, C. Rolland, G. Tronchin, J.P. Latgé, S. Paris, *rodletless* mutants of *Aspergillus fumigatus*, Infect. Immun. 62(10) (1994) 4380–4388.
[15] H. Liu, M.J. Lee, N.V. Solis, Q.T. Phan, M. Swidergall, B. Ralph, A.S. Ibrahim, D.C. Sheppard, S.G. Filler, *Aspergillus fumigatus* CalA binds to integrin α5β1 and mediates host cell invasion, Nat. Microbiol. 2 (2016) 16211.
[16] J. Amich, R. Vicentefranqueira, F. Leal, J.A. Calera, *Aspergillus fumigatus* survival in alkaline and extreme zinc-limiting environments relies on the induction of a zinc homeostasis system encoded by the *zrfC* and *aspf2* genes, Eukaryot. Cell 9(3) (2010) 424–437.
[17] B. Banerjee, P.A. Greenberger, J.N. Fink, V.P. Kurup, Immunological characterization of Asp f 2, a major allergen from *Aspergillus fumigatus* associated with allergic bronchopulmonary aspergillosis, Infect. Immun. 66(11) (1998) 5175–5182.
[18] P. Dasari, I.A. Shopova, M. Stroe, D. Wartenberg, H. Martin-Dahse, N. Beyersdorf, P. Hortschansky, S. Dietrich, Z. Cseresnyés, M.T. Figge, M. Westermann, C. Skerka, A.A. Brakhage, P.F. Zipfel, Aspf2 from *Aspergillus fumigatus* recruits human immune regulators for immune evasion and cell damage, Front. Immunol. 9 (2018) 1635.
[19] A.R. Asif, M. Oellerich, V.W. Amstrong, B. Riemenschneider, M. Monod, U. Reichard, Proteome of conidial surface associated proteins of *Aspergillus fumigatus* reflecting potential vaccine candidates and allergens, J. Proteome Res. 5(4) (2006) 954–962.
[20] J. Esbelin, T. Santos, C. Ribière, M. Desvaux, D. Viala, C. Chambon, M. Hébraud, Comparison of three methods for cell surface proteome extraction of *Listeria monocytogenes* biofilms, OMICS 22(12) (2018) 779–787.
[21] C. Urban, K. Sohn, F. Lottspeich, H. Brunner, S. Rupp, Identification of cell surface determinants in *Candida albicans* reveals Tsa1p, a protein differentially localized in the cell, FEBS Lett. 544(1-3) (2003) 228–235.

[22] N. de Miguel, G. Lustig, O. Twu, A. Chattopadhyay, J.A. Wohlschlegel, P.J. Johnson, Proteome analysis of the surface of *Trichomonas vaginalis* reveals novel proteins and strain-dependent differential expression, Mol. Cell. Proteomics 9(7) (2010) 1554–1566.
[23] D. Wessel, U.I. Flügge, A method for the quantitative recovery of protein in dilute solution in the presence of detergents and lipids, Anal. Biochem. 138(1) (1984) 141–143.
[24] K. Lapp, M. Vödisch, K. Kroll, M. Strassburger, O. Kniemeyer, T. Heinekamp, A.A. Brakhage, Characterization of the *Aspergillus fumigatus* detoxification systems for reactive nitrogen intermediates and their impact on virulence, Front. Microbiol. 5 (2014) 469.
[25] M.E. da Silva Ferreira, M.R. Kress, M. Savoldi, M.H. Goldman, A. Härtl, T. Heinekamp, A.A. Brakhage, G.H. Goldman, The *akuB*(KU80) mutant deficient for nonhomologous end joining is a powerful tool for analyzing pathogenicity in *Aspergillus fumigatus*, Eukaryot. Cell 5(1) (2006) 207–211.
[26] Y. Perez-Riverol, A. Csordas, J. Bai, M. Bernal-Llinares, S. Hewapathirana, D.J. Kundu, A. Inuganti, J. Griss, G. Mayer, M. Eisenacher, E. Pérez, J. Uszkoreit, J. Pfeuffer, T. Sachsenberg, S. Yilmaz, S. Tiwary, J. Cox, E. Audain, M. Walzer, A.F. Jarnuczak, T. Ternent, A. Brazma, J.A. Vízcaino, The PRIDE database and related tools and resources in 2019: improving support for quantification data, Nucleic Acids Res. 47(D1) (2019) D442–D450.
[27] G. Elia, Biotinylation reagents for the study of cell surface proteins, Proteomics 8(19) (2008) 4012–4024.
[28] E.Y. Basenko, J.A. Pulman, A. Shanmugasundram, O.S. Harb, K. Crouch, D. Starns, S. Warrenfeltz, C. Aurrecoechea, C.J. Stoeckert, Jr., J.C. Kissinger, D.S. Roos, C. Hertz-Fowler, FungiDB: An integrated bioinformatic resource for fungi and oomycetes, J. Fungi 4(1) (2018) 39.
[29] J. Teutschbein, D. Albrecht, M. Pötsch, R. Guthke, V. Aimanianda, C. Clavaud, J.P. Latgé, A.A. Brakhage, O. Kniemeyer, Proteome profiling and functional classification of intracellular proteins from conidia of the human-pathogenic mold *Aspergillus fumigatus*, J. Proteome Res. 9(7) (2010) 3427–3442.
[30] A. Beauvais, M. Monod, J.P. Debeaupuis, M. Diaquin, H. Kobayashi, J.P. Latgé, Biochemical and antigenic characterization of a new dipeptidyl-peptidase isolated from *Aspergillus fumigatus*, J. Biol. Chem. 272(10) (1997) 6238–6244.
[31] I. Mouyna, R.P. Hartland, T. Fontaine, M. Diaquin, C. Simenel, M. Delepierre, B. Henrissat, J.P. Latgé, A 1,3-beta-glucanosyltransferase isolated from the cell wall of *Aspergillus fumigatus* is a homologue of the yeast Bgl2p, Microbiology 144 (Pt 11) (1998) 3171–3180.
[32] A. Gastebois, I. Mouyna, C. Simenel, C. Clavaud, B. Coddeville, M. Delepierre, J.P. Latgé, T. Fontaine, Characterization of a new beta(1-3)-glucan branching activity of *Aspergillus fumigatus*, J. Biol. Chem. 285(4) (2010) 2386–2396.
[33] F.N. Gravelat, D.E. Ejzykowicz, L.Y. Chiang, J.C. Chabot, M. Urb, K.D. Macdonald, N. al-Bader, S.G. Filler, D.C. Sheppard, *Aspergillus fumigatus* MedA governs adherence, host cell interactions and virulence, Cell. Microbiol. 12(4) (2010) 473–488.
[34] F. Lamoth, P.R. Juvvadi, E.J. Soderblom, M.A. Moseley, W.J. Steinbach, Hsp70 and the Cochaperone StiA (Hop) Orchestrate Hsp90-Mediated Caspofungin Tolerance in *Aspergillus fumigatus*, Antimicrob. Agents Chemother. 59(8) (2015) 4727–4733.
[35] A.R. Asif, M. Oellerich, V.W. Amstrong, U. Gross, U. Reichard, Analysis of the cellular *Aspergillus fumigatus* proteome that reacts with sera from rabbits developing an acquired immunity after experimental aspergillosis, Electrophoresis 31(12) (2010) 1947–1958.

662 [36] B. Singh, M. Oellerich, R. Kumar, M. Kumar, D.P. Bhadoria, U. Reichard, V.K. Gupta,
663 G.L. Sharma, A.R. Asif, Immuno-reactive molecules identified from the secreted proteome of
664 *Aspergillus fumigatus*, J. Proteome Res. 9(11) (2010) 5517–5529.
665 [37] B. Singh, G.L. Sharma, M. Oellerich, R. Kumar, S. Singh, D.P. Bhadoria, A. Katyal, U.
666 Reichard, A.R. Asif, Novel cytosolic allergens of *Aspergillus fumigatus* identified from
667 germinating conidia, J. Proteome Res. 9(11) (2010) 5530–5541.
668 [38] R. Rosenzweig, N.B. Nillegoda, M.P. Mayer, B. Bukau, The Hsp70 chaperone network,
669 Nat. Rev. Mol. Cell Biol. 20(11) (2019) 665–680.
670 [39] A. De Maio, D. Vazquez, Extracellular heat shock proteins: a new location, a new function,
671 Shock 40(4) (2013) 239–246.
672 [40] T. Akoumianaki, I. Kyrmizi, I. Valsecchi, M.S. Gresnigt, G. Samonis, E. Drakos, D.
673 Boumpas, L. Muszkieta, M.C. Prevost, D.P. Kontoyiannis, T. Chavakis, M.G. Netea, F.L. van de
674 Veerdonk, A.A. Brakhage, J. El-Benna, A. Beauvais, J.P. Latgé, G. Chamilos, *Aspergillus* cell
675 wall melanin blocks LC3-associated phagocytosis to promote pathogenicity, Cell Host Microbe.
676 19(1) (2016) 79–90.
677 [41] I. Kyrmizi, H. Ferreira, A. Carvalho, J.A.L. Figueroa, P. Zarmpas, C. Cunha, T.
678 Akoumianaki, K. Stylianou, G.S. Deepe, Jr., G. Samonis, J.F. Lacerda, A. Campos, Jr., D.P.
679 Kontoyiannis, N. Mihalopoulos, K.J. Kwon-Chung, J. El-Benna, I. Valsecchi, A. Beauvais, A.A.
680 Brakhage, N.M. Neves, J.P. Latgé, G. Chamilos, Calcium sequestration by fungal melanin
681 inhibits calcium-calmodulin signalling to prevent LC3-associated phagocytosis, Nat. Microbiol.
682 3 (2018) 791–803.
683 [42] S.E. Cagas, M.R. Jain, H. Li, D.S. Perlin, Profiling the *Aspergillus fumigatus* proteome in
684 response to caspofungin, Antimicrob. Agents Chemother. 55(1) (2011) 146–154.
685 [43] A.J. Foster, R.A. Bird, S.N. Smith, Biotinylation and characterization of *Cryptococcus*
686 *neoformans* cell surface proteins, J. Appl. Microbiol. 103(2) (2007) 390–399.
687 [44] E.M. Conn, M.A. Madsen, B.F. Cravatt, W. Ruf, E.I. Deryugina, J.P. Quigley, Cell surface
688 proteomics identifies molecules functionally linked to tumor cell intravasation, J. Biol. Chem.
689 283(39) (2008) 26518–26527.
690 [45] H. Schmidt, S. Vlaic, T. Krüger, F. Schmidt, J. Balkenhol, T. Dandekar, R. Guthke, O.
691 Kniemeyer, T. Heinekamp, A.A. Brakhage, Proteomics of *Aspergillus fumigatus* conidia-
692 containing phagolysosomes identifies processes governing immune evasion, Mol. Cell.
693 Proteomics 17(6) (2018) 1084–1096.
694 [46] J.D. Crowe, I.K. Sievwright, G.C. Auld, N.R. Moore, N.A. Gow, N.A. Booth, *Candida*
695 *albicans* binds human plasminogen: identification of eight plasminogen-binding proteins, Mol.
696 Microbiol. 47(6) (2003) 1637–1651.
697 [47] P.R. Kraus, A.F. Hofmann, S.D. Harris, Characterization of the *Aspergillus nidulans* 14-3-3
698 homologue, ArtA, FEMS Microbiol. Lett. 210(1) (2002) 61–66.
699 [48] B.A. Ibarra, J.M. Lohmar, T. Satterlee, T. McDonald, J.W. Cary, A.M. Calvo, The 14-3-3
700 protein homolog ArtA regulates development and secondary metabolism in the opportunistic
701 plant pathogen *Aspergillus flavus*, Appl. Environ. Microbiol. 84(5) (2018) e02241-17.
702 [49] E.K. Brauer, N. Manes, C. Bonner, R. Subramaniam, Two 14-3-3 proteins contribute to
703 nitrogen sensing through the TOR and glutamine synthetase-dependent pathways in *Fusarium*
704 *graminearum*, Fungal Genet. Biol. 134 (2020) 103277.
705 [50] X.S. Li, J.N. Sun, K. Okamoto-Shibayama, M. Edgerton, *Candida albicans* cell wall ssa
706 proteins bind and facilitate import of salivary histatin 5 required for toxicity, J. Biol. Chem.
707 281(32) (2006) 22453–22463.

[51] C.P. Silveira, A.C. Piffer, L. Kmetzsch, F.L. Fonseca, D.A. Soares, C.C. Staats, M.L. Rodrigues, A. Schrank, M.H. Vainstein, The heat shock protein (Hsp) 70 of *Cryptococcus neoformans* is associated with the fungal cell surface and influences the interaction between yeast and host cells, Fungal Genet. Biol. 60 (2013) 53–63.
[52] L. Neckers, U. Tatu, Molecular chaperones in pathogen virulence: emerging new targets for therapy, Cell Host Microbe. 4(6) (2008) 519–527.
[53] S. Nair, E. Milohanic, P. Berche, ClpC ATPase is required for cell adhesion and invasion of *Listeria monocytogenes*, Infect. Immun. 68(12) (2000) 7061–7068.
[54] C. Rouquette, C. de Chastellier, S. Nair, P. Berche, The ClpC ATPase of *Listeria monocytogenes* is a general stress protein required for virulence and promoting early bacterial escape from the phagosome of macrophages, Mol. Microbiol. 27(6) (1998) 1235–1245.
[55] J.N. Sun, N.V. Solis, Q.T. Phan, J.S. Bajwa, H. Kashleva, A. Thompson, Y. Liu, A. Dongari-Bagtzoglou, M. Edgerton, S.G. Filler, Host cell invasion and virulence mediated by *Candida albicans* Ssa1, PLoS Pathog. 6(11) (2010) e1001181.
[56] R. Hooft van Huijsduijnen, S. Kojima, D. Carter, H. Okabe, A. Sato, W. Akahata, T.N.C. Wells, K. Katsuno, Reassessing therapeutic antibodies for neglected and tropical diseases, PLoS Negl. Trop. Dis. 14(1) (2020) e0007860.
[57] R.C. Matthews, G. Rigg, S. Hodgetts, T. Carter, C. Chapman, C. Gregory, C. Illidge, J. Burnie, Preclinical assessment of the efficacy of mycograb, a human recombinant antibody against fungal HSP90, Antimicrob. Agents Chemother. 47(7) (2003) 2208–2216.
[58] L. Thomaz, J.D. Nosanchuk, D.C.P. Rossi, L.R. Travassos, C.P. Taborda, Monoclonal antibodies to heat shock protein 60 induce a protective immune response against experimental *Paracoccidioides lutzii*, Microbes Infect. 16(9) (2014) 788–795.
[59] A.J. Guimarães, S. Frases, F.J. Gomez, R.M. Zancopé-Oliveira, J.D. Nosanchuk, Monoclonal antibodies to heat shock protein 60 alter the pathogenesis of *Histoplasma capsulatum*, Infect. Immun. 77(4) (2009) 1357–1367.
[60] F. Hillmann, K. Bagramyan, M. Straßburger, T. Heinekamp, T.B. Hong, K.P. Bzymek, J.C. Williams, A.A. Brakhage, M. Kalkum, The crystal structure of peroxiredoxin Asp f3 provides mechanistic insight into oxidative stress resistance and virulence of *Aspergillus fumigatus*, Sci. Rep. 6 (2016) 33396.
[61] A.G. Glaser, A. Limacher, F. S., A. Scheynius, L. Scapozza, R. Crameri, Analysis of the cross-reactivity and of the 1.5 Å crystal structure of the *Malassezia sympodialis* Mala s 6 allergen, a member of the cyclophilin pan-allergen family, Biochem. J. 396(1) (2006) 41–49.
[62] T.E. Twaroch, M. Curin, R. Valenta, I. Swoboda, Mold allergens in respiratory allergy: from structure to therapy, Allergy Asthma Immunol. Res. 7(3) (2015) 205–220.
[63] G. Sircar, M. Bhowmik, R.K. Sarkar, N. Najafi, A. Dasgupta, M. Focke-Tejkl, S. Flicker, I. Mittermann, R. Valenta, K. Bhattacharya, S. Gupta Bhattacharya, Molecular characterization of a fungal cyclophilin allergen Rhi o 2 and elucidation of antigenic determinants responsible for IgE-cross-reactivity, J. Biol. Chem. 295(9) (2020) 2736–2748.
[64] P. San Segundo-Acosta, C. Oeo-Santos, S. Benedé, V. de Los Ríos, A. Navas, B. Ruiz-Leon, C. Moreno, C. Pastor-Vargas, A. Jurado, M. Villalba, R. Barderas, Delineation of the olive pollen proteome and its allergenome unmasks cyclophilin as a relevant cross-reactive allergen, J. Proteome Res. 18(8) (2019) 3052–3066.

Table S1. *A. fumigatus* strains used in this study.

Description	Relevant genotype	Reference or source
Wild type	CEA10	Fungal Genetics Stock Center (A1163)
A1160	Δ*ku80* pyrG^{+}	da Silva Ferreira et al., 2006 [25]
hsp70-Myc	A1160 *hsp70-Myc-ptrA*; PT^{R}	This study
ssc70-Myc	A1160 *ssc70-Myc-ptrA*; PT^{R}	This study
bipA-Myc	A1160 *bipA-Myc-ptrA*; PT^{R}	This study
ssz-Myc	A1160 *ssz-Myc-ptrA*; PT^{R}	This study

752

753 **Table S2**. Oligonucleotides used in this study.

Name	Sequence 5' to 3'	Usage
Ssc70-M_F	TTCGAGCTCGGTACCTTCTCGGAATGACATTAAGC	Plasmid pLJ-Ssc70-Myc
Ssc70-M_R	AAGATCCTCCTCGGAGATAAGCTTCTGCTCGGGCTTGTTCTCACCCTG	
Myc_F	ATCTCCGAGGAGGATCTTGGCTCCGGCTCCTAAAGCGGCCGCCCGGCTGC	
pTH_R	CCTGAGTGGCCATCGAATTC	
Hsp70-M_F	TTCGAGCTCGGTACCTGAGAGAGCCGAGGGCTACG	Plasmid pLJ-Hsp70-Myc
Hsp70-M_R	CCTCCTCGGAGATAAGCTTCTGCTCGTCAAGCTCCTCAGGGCGCT	
BipA-M_F	TTCGAGCTCGGTACCCCCGAGTACATTGATAGAGG	Plasmid pLJ-BipA-Myc
BipA-M_R	CTCGGAGATAAGCTTCTGCTCCAGTTCGTCATGTCCGCTGG	
Ssz-M_F	TTCGAGCTCGGTACCCCTCCGTTCAATGGGCCCAA	Plasmid pLJ-Ssz-Myc
Ssz-M_R	CTCGGAGATAAGCTTCTGCTCAGCCTTGGGCGACTCGACGG	

754

Figure 1

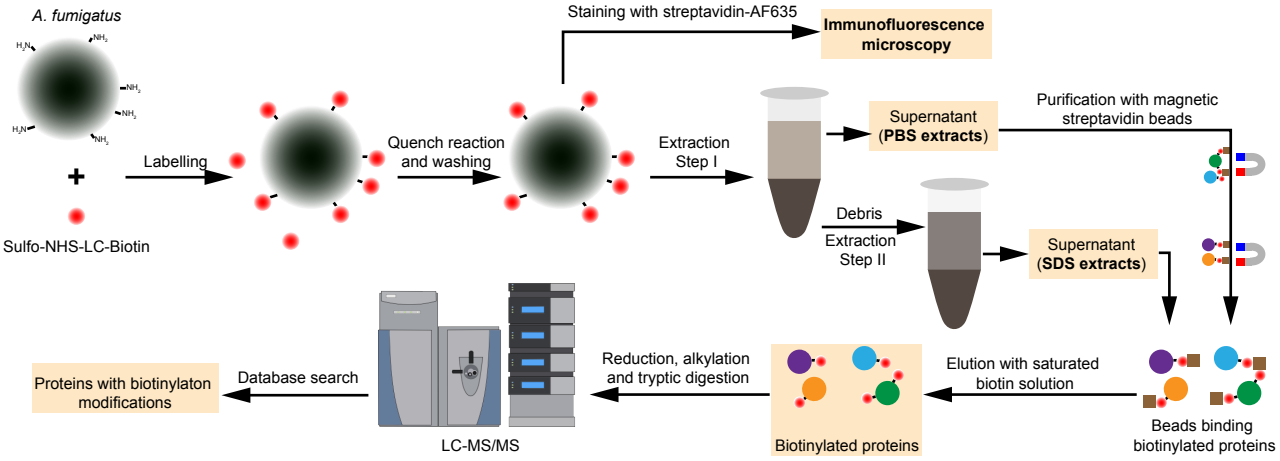

Figure 2

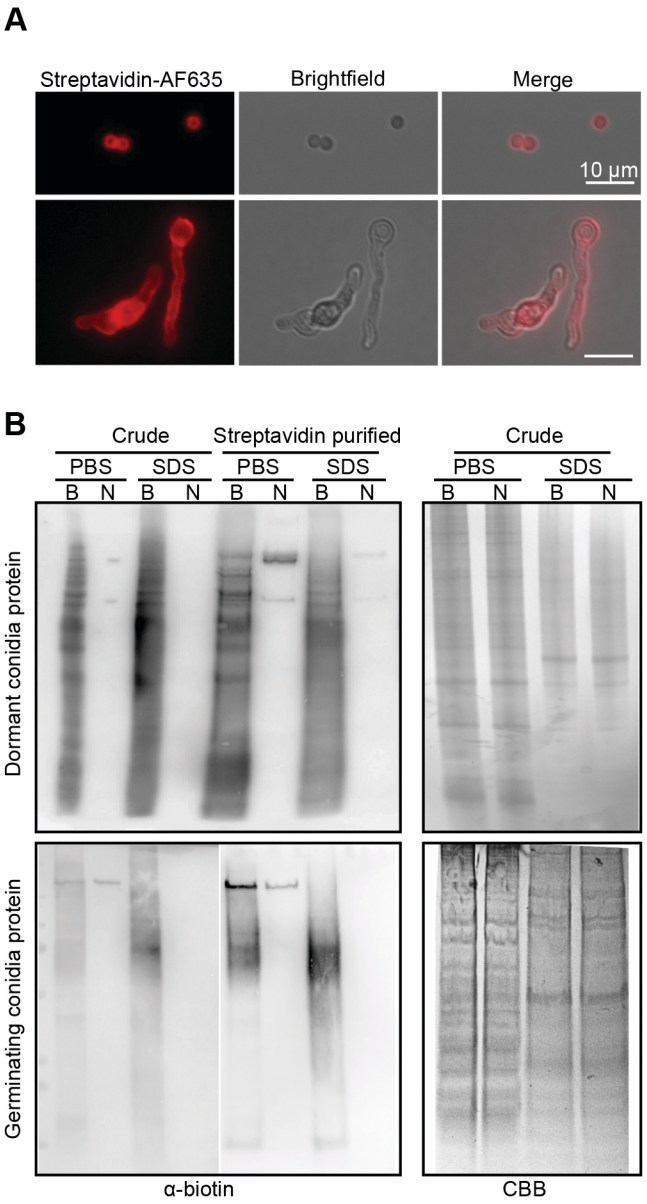

Figure 3

A

Samples	Total protein[a]		Biotinylated protein[b]	
	PBS	SDS	PBS	SDS
DC	518	362	60	21
SC	550	269	69	11
GC	618	247	88	8
M	486	178	202	53
Sum	**1139**		**314**	

B

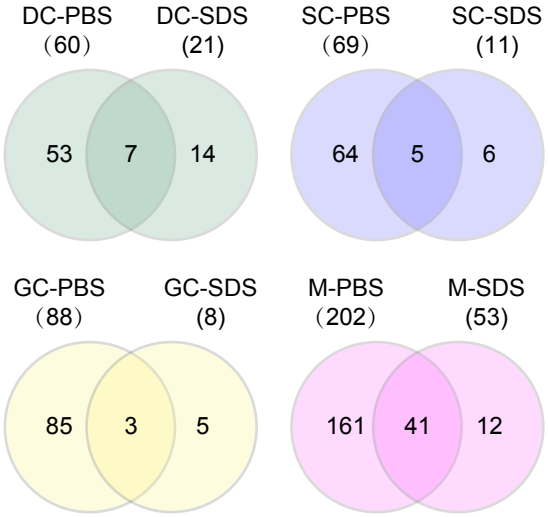

C

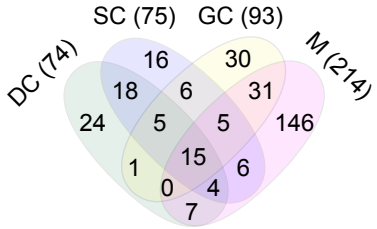

Figure 4

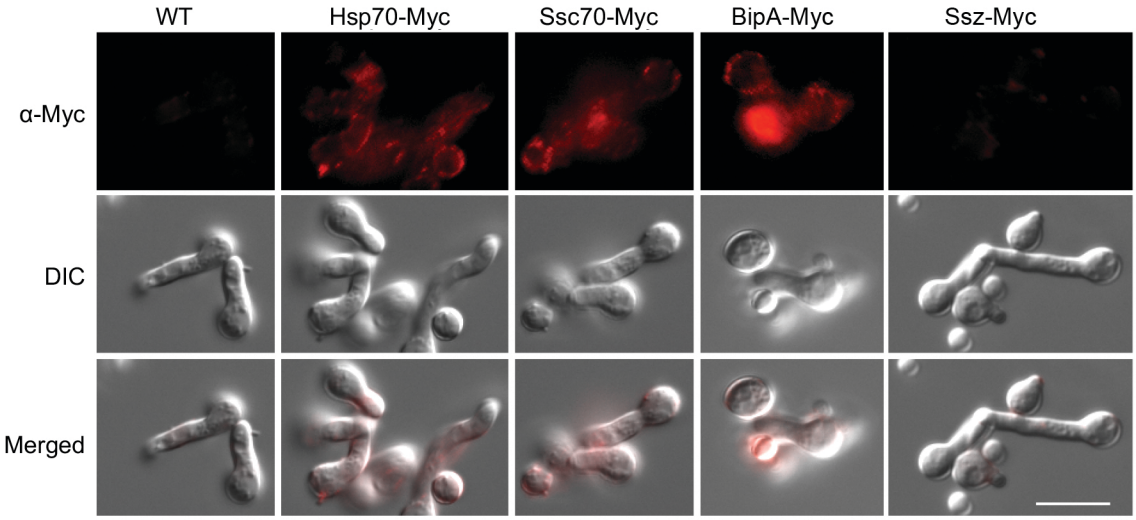

Figure 5

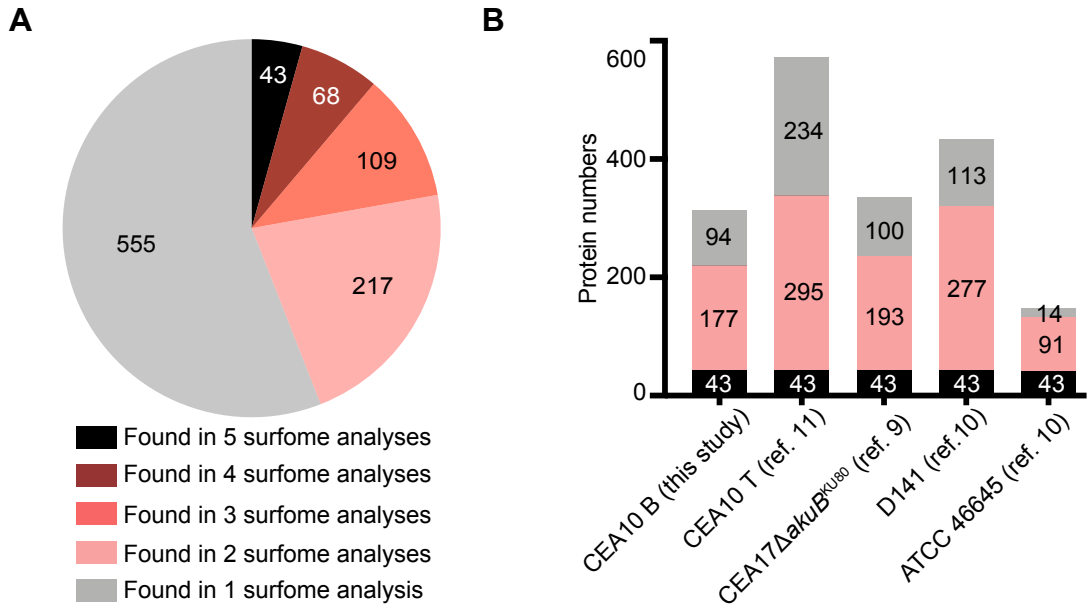

Figure S1

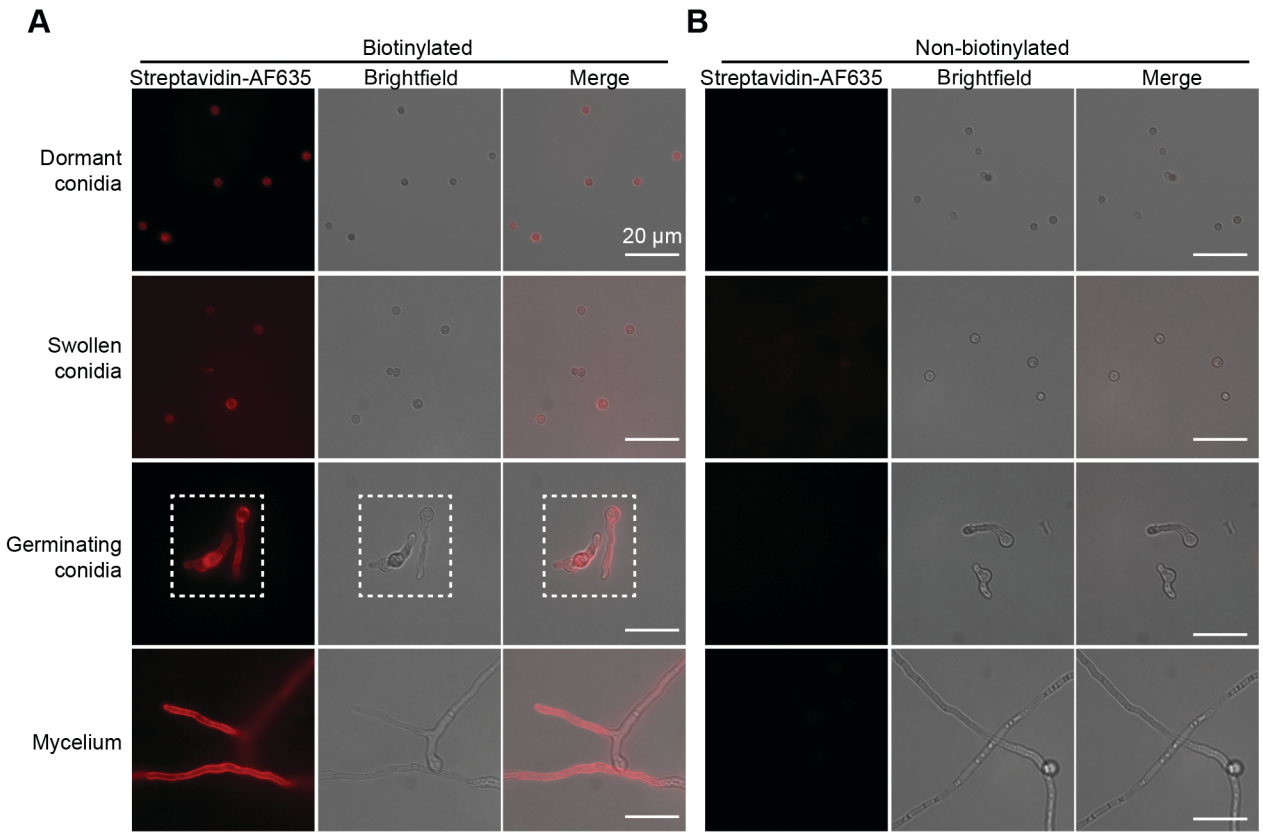

Figure S2

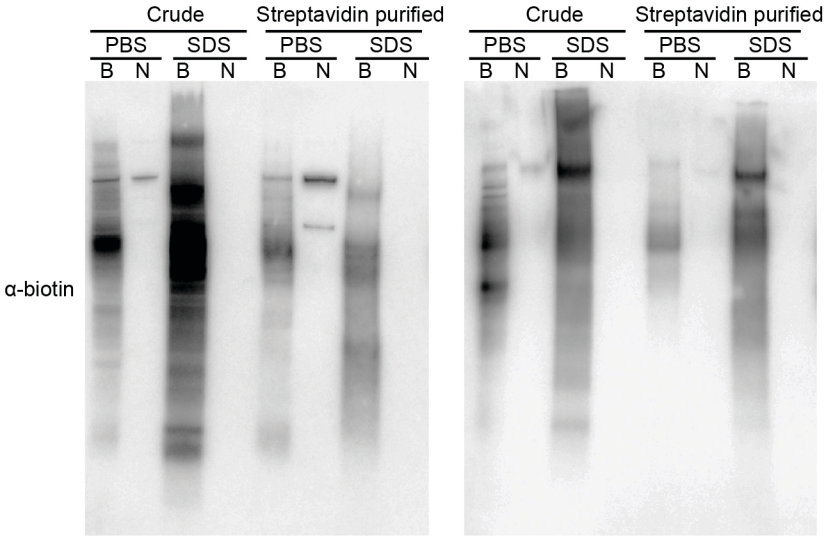

Figure S3

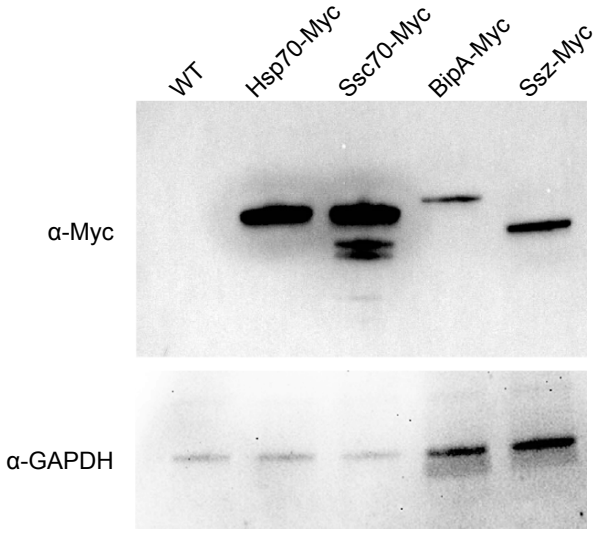

Figure S4